Impact of Time Delays on Power System Stability

F. Milano, *Senior Member, IEEE* and M. Anghel

***Abstract*— The paper describes the impact of time-delays on small-signal angle stability of power systems. With this aim, the paper presents a power system model based on delay differential algebraic equations (DDAE) and describes a general technique for computing the spectrum of DDAE. The paper focuses in particular on delays due to the terminal voltage measurements and transducers of automatic voltage regulators and power system stabilizers of synchronous machines. The proposed technique is applied to a benchmark system, namely the IEEE 14-bus test system, as well as to a real-world system. Time domain simulations are also presented to confirm the results of the DDAE spectral analysis.**

***Index Terms*— Time delay, delay differential algebraic equations (DDAE), automatic voltage regulator (AVR), power system stabilizer (PSS), small-signal stability, Hopf bifurcation (HB), limit cycle.**

I. Introduction

A. Motivation

Including time delays in the classical electromechanical model leads to formulating power systems in terms of functional differential algebraic equations of retarded type or, more concisely, delay differential algebraic equations (DDAE). The study of the stability of DDAE is relatively more complicated than that of standard differential algebraic equations (DAE). Nevertheless, both theoretical tools for DDAE and modern computers are mature enough to allow tackling the stability of large scale DDAE systems. This paper presents a systematic approach for defining small signal stability as well as time domain integration of power systems modeled as DDAE.

B. Literature Review

Time delays arises in a wide variety of physical systems and their effects on stability have been carefully investigated in several engineering applications, such as signal processing and circuit design [1]–[4]. Nevertheless, little work has been carried out so far in the power system area on the effects of time delays on power system stability. As a matter of fact, time delays are generally ignored. An exception to this rule is [5], which presents a model of long transmission lines in terms of DDAE.

In recent years, wide measurement areas and recent applications of phasor measurement unit (PMU) devices make necessary remote measures, which has led to some research on the effect of measurement delays. For example, [6] and [7] present a robust control of time delays for wide-area power system stabilizers, and [8] tackles the issue of the time domain integration of DDAE. The effect on small signal stability of delays due to PMU measurements are studied in [9] based on a probabilistic approach.

Existing studies on small-signal stability of delayed power system equations can be divided into two main categories: (i) frequency-domain methods, and (ii) time-domain methods.

1) Frequency-domain methods: These methods mainly consists in the evaluation of the roots of the characteristic equation of the retarded system [9]–[11]. This approach is in principle exact but due to the difficulty in determining the roots of the characteristic equation (see Section II-A), the analysis is limited to one-machine infinite-bus (OMIB) systems.

Although an exact explicit analytical method based on the Lambert W function can be applied to simple cases [12], the analytical solution of the characteristic equation cannot be found for practical power systems. Thus, several numerical methods have been proposed in the literature to approximate the solution of the characteristic equation. A possible approach is based on the discretization of the solution operator of the characteristic equation [13]. Other methods estimate the infinitesimal generator of the solution operator semi-group [14], and the solution operator approach via linear multistep (LMS) time integration of retarded systems without any distributed delay term [15]–[17].

Other approaches apply a discretization scheme based on Chebyshev's nodes [18]–[20]. These methods are based on a discretization of the partial differential equation (PDE) representation of the DDAE. The implementation of such discretization is surprisingly simple while results proved to be accurate. Hence, this is the technique used in this paper. The idea is to transform the original DDAE problem into an equivalent PDE system of infinite dimensions. Then, instead of computing the roots of retarded functional differential equations, one has to solve a finite, though possibly large, matrix eigenvalue problem of the discretized PDE system.

2) Time-domain methods: These methods are based on the Lyapunov-Krasovskii's stability theorem and the Razumikhin's theorem. The application of time-domain methods allow defining robust controllers (e.g., H_∞ control) and dealing with uncertainties and time-varying delays. However, the conditions of the Lyapunov-Krasovskii's stability theorem and the Razumikhin's theorem are only sufficient and cannot be used to find the delay stability margin. Moreover, it is necessary to

F. Milano is with the Department of Electrical Engineering, University of Castilla-La Mancha, 13071 Ciudad Real, Spain. E-mail: Federico.Milano@uclm.es.

M. Anghel is with CCS Division, Los Alamos National Laboratory, Los Alamos, NM 87545, USA. E-mail:manghel@lanl.gov.

Federico Milano is partly supported by the Ministry of Science and Education of Spain through CICYT Project ENE-2009-07685 and by Junta de Comunidades de Castilla - La Mancha through project PCI-08-0102.

Marian Anghel research was carried out under the auspices of the National Nuclear Security Administration of the U.S. Department of Energy at Los Alamos National Laboratory under Contract No. DE C52-06NA25396.

find a Lyapunov functional or, according to the Razumikhin's theorem, a Lyapunov function that bounds the Lyapunov functional.

Hence, in the nonlinear case, the applicability of time-domain methods strongly depends on the ability of defining a Lyapunov function (i.e., the same limitation as DAE systems). The application to power system analysis are limited to small test systems [21], [22].

If the DDAE is linear or is linearized around an equilibrium point, finding the Lyapunov function, in turns, implies finding a solution of a linear matrix inequality (LMI) problem [23], [24]. A drawback of this approach is that the size and the computational burden of LMI highly increase with the size of the DDAE. As a matter of fact, LMI-based analysis has become computationally tractable only in the last two decades [24]. However, in recent years, LMI-based approach has been applied to several practical problems. In the scope of power system analysis, we cite, for example, [25].

3) Advantages and drawbacks of frequency- and time-domain methods: As discussed above, the frequency and the time-domain methods have both advantages and drawbacks, which have to be carefully evaluated in order to define the best application of each method. While time-domain methods are adequate for synthesizing robust controllers, as any direct method based on the Lyapunov function, they suffer from the idiosyncratic lack of necessary and sufficient stability conditions. Furthermore, the computational burden of solving the LMI problem cannot be avoided.

On the other hand, while it is true that frequency-domain methods have difficulties in handling uncertainties, they offer the advantage of consisting in an eigenvalue analysis of a (possibly huge) matrix. If one is interested in stability, the object is not to find *all* roots, but only a reduced set of roots that have positive real part of that are close to the imaginary axis. Some efficient eigenvalue technique, e.g., the Arnoldi's iteration, can highly reduce the computational burden of frequency-domain techniques.

For these reasons, and since in this paper we are interested in the small-signal analysis of DDAE more than in its robust control, we use the frequency-domain approach.

C. Object of the Paper

In this paper, we are interested in determining whether the inclusion of delays can affect the small-signal stability and whether such delays can reduce the expected stability margin of a power system. Both mathematical and computational aspects are taken into account so that the proposed procedures for small-signal analysis as well as for time domain integration can be in principle applied to a power system of any size and complexity. Moreover, we show that the implementation of ideal constant delays is particularly straightforward and does not affect the numerical stability of the implicit trapezoidal method that is used in most power system analysis software tools.

D. Contributions

The contributions of the paper are the following:

1) To define a general DDAE model of power systems. In particular, the index-1 Hessenberg form of retarded type is adopted.
2) To propose a method for defining the small-signal stability of DDAE based on eigenvalue analysis and an approximation of the characteristic equation at equilibrium points.
3) To evaluate the effect on stability of taking into account delays in measurements. With this aim, the case study considers delays introduced by the excitation control as well as by the power system stabilizer of synchronous machines.

E. Paper Organization

The remainder of the paper is organized as follows. Section II defines the structure of DDAE that is adequate for power system modeling. Subsection II-A proposes a technique for evaluating the small-signal stability of DDAE equilibrium points based on an approximate solution of the characteristic equation while Subsection II-B describes the modifications required by the implicit trapezoidal method for integrating DDAE. Section III presents the AVR model with inclusion of a time delay. Section IV discusses simulation results obtained for the IEEE 14-bus test system and a real-world 1213-bus system. Conclusions are drawn in Section V.

II. DDAE for Power System Modeling

The transient behavior of electric power systems is traditionally described through a set of differential algebraic equations (DAE) as follows:

$$\begin{aligned} \dot{\boldsymbol{x}} &= \boldsymbol{f}(\boldsymbol{x}, \boldsymbol{y}, \boldsymbol{u}) \\ \mathbf{0} &= \boldsymbol{g}(\boldsymbol{x}, \boldsymbol{y}, \boldsymbol{u}) \end{aligned} \tag{1}$$

where $\boldsymbol{f}$ ($\boldsymbol{f} : \mathbb{R}^{n+m+p} \mapsto \mathbb{R}^n$) are the differential equations, $\boldsymbol{g}$ ($\boldsymbol{g} : \mathbb{R}^{n+m+p} \mapsto \mathbb{R}^m$) are the algebraic equations, $\boldsymbol{x}$ ($\boldsymbol{x} \in \mathbb{R}^n$) are the state variables, $\boldsymbol{y}$ ($\boldsymbol{y} \in \mathbb{R}^m$) are the algebraic variables, and $\boldsymbol{u}$ ($\boldsymbol{u} \in \mathbb{R}^p$) are discrete variables modeling events, e.g., line outages and faults.

In common practice, equations (1) are split into a collection of subsystems where discrete variables $\boldsymbol{u}$ are substituted for *if-then* rules. Thus, (1) can be conveniently rewritten as a finite collection of continuous DAEs, one per each discrete variable change. Such a system is also known as *hybrid automaton* or *hybrid dynamical system*. An in-depth description and formalization of hybrid systems for power system analysis can be found in [26].

Despite the fact that (1) are well-accepted and are the common choice in power system software packages, some aspects of the reality are missing from this formulation, e.g., stochastic processes and variable functional relations. In this paper, we are interested in defining the possible effects on stability of time delays. Introducing time delays in (1) changes the DAE into a set of delay differential algebraic equations (DDAE). For the sake of simplicity, we only consider ideal constant time delays in the form:

$$y_d = y(t - \tau) \tag{2}$$

where y_d is the *retarded* or *delayed* variable with respect to some algebraic variable y, t is the current simulation time, and τ ($\tau > 0$) is the constant delay. A similar expression, with obvious notation, can be written in case the delay affects a state variable:

$$x_d = x(t - \tau) \tag{3}$$

Merging together (1), (2) and (3) leads to:

$$\begin{aligned} \dot{\boldsymbol{x}} &= \boldsymbol{f}(\boldsymbol{x}, \boldsymbol{y}, \boldsymbol{x}_d, \boldsymbol{y}_d, \boldsymbol{u}) \\ \boldsymbol{0} &= \boldsymbol{g}(\boldsymbol{x}, \boldsymbol{y}, \boldsymbol{x}_d, \boldsymbol{y}_d, \boldsymbol{u}) \end{aligned} \tag{4}$$

Equations (4) are the most general form of nonlinear DDAE. However, for practical models of physical systems, some simplifications can be adopted. In particular, as shown in Section III, the index-1 Hessenberg form is adequate to model power systems:

$$\begin{aligned} \dot{\boldsymbol{x}} &= \boldsymbol{f}(\boldsymbol{x}, \boldsymbol{y}, \boldsymbol{x}_d, \boldsymbol{y}_d, \boldsymbol{u}) \\ \boldsymbol{0} &= \boldsymbol{g}(\boldsymbol{x}, \boldsymbol{y}, \boldsymbol{x}_d, \boldsymbol{u}) \end{aligned} \tag{5}$$

which is a simplification of (4). The index-1 Hessenberg form (5) is used in the remainder of the paper.

In this paper, we are interested in (i) defining the small-signal stability of (5), and (ii) numerically integrating (5). These topics are addressed in the following subsections.

A. Small-Signal Stability of Hessenberg DDAE of Retarded Type

Assume that a stationary solution of (5) is known and has the form:

$$\begin{aligned} \boldsymbol{0} &= \boldsymbol{f}(\boldsymbol{x}_0, \boldsymbol{y}_0, \boldsymbol{x}_0, \boldsymbol{y}_0, \boldsymbol{u}_0) \\ \boldsymbol{0} &= \boldsymbol{g}(\boldsymbol{x}_0, \boldsymbol{y}_0, \boldsymbol{x}_0, \boldsymbol{u}_0) \end{aligned} \tag{6}$$

Then, linearizing (5) at the stationary solution yields:

$$\Delta\dot{\boldsymbol{x}} = \boldsymbol{f}_{\boldsymbol{x}}\Delta\boldsymbol{x} + \boldsymbol{f}_{\boldsymbol{x}_d}\Delta\boldsymbol{x}_d + \boldsymbol{f}_{\boldsymbol{y}}\Delta\boldsymbol{y} + \boldsymbol{f}_{\boldsymbol{y}_d}\Delta\boldsymbol{y}_d \tag{7}$$

$$\boldsymbol{0} = \boldsymbol{g}_{\boldsymbol{x}}\Delta\boldsymbol{x} + \boldsymbol{g}_{\boldsymbol{x}_d}\Delta\boldsymbol{x}_d + \boldsymbol{g}_{\boldsymbol{y}}\Delta\boldsymbol{y} \tag{8}$$

where, as usual, it can be assumed that $\boldsymbol{g}_{\boldsymbol{y}}$ is non-singular. Thus, substituting (8) into (7), one obtains:

$$\Delta\dot{\boldsymbol{x}} = \boldsymbol{A}_0\Delta\boldsymbol{x} + \boldsymbol{A}_1\Delta\boldsymbol{x}(t-\tau) + \boldsymbol{A}_2\Delta\boldsymbol{x}(t-2\tau) \tag{9}$$

where:

$$\boldsymbol{A}_0 = \boldsymbol{f}_{\boldsymbol{x}} - \boldsymbol{f}_{\boldsymbol{y}}\boldsymbol{g}_{\boldsymbol{y}}^{-1}\boldsymbol{g}_{\boldsymbol{x}} \tag{10}$$

$$\boldsymbol{A}_1 = \boldsymbol{f}_{\boldsymbol{x}_d} - \boldsymbol{f}_{\boldsymbol{y}}\boldsymbol{g}_{\boldsymbol{y}}^{-1}\boldsymbol{g}_{\boldsymbol{x}_d} - \boldsymbol{f}_{\boldsymbol{y}_d}\boldsymbol{g}_{\boldsymbol{y}}^{-1}\boldsymbol{g}_{\boldsymbol{x}} \tag{11}$$

$$\boldsymbol{A}_2 = -\boldsymbol{f}_{\boldsymbol{y}_d}\boldsymbol{g}_{\boldsymbol{y}}^{-1}\boldsymbol{g}_{\boldsymbol{x}_d} \tag{12}$$

The first matrix $\boldsymbol{A}_0$ is the well-known state matrix that is computed for standard DAE system of the form (1). The other two matrices are not null only if the system is of retarded type Appendix I provides the details on how to determine (10)-(12). Observe that (9) is equivalent to the linearization of the DDE system obtained by substituting y for a function $\boldsymbol{y} = \boldsymbol{\rho}(\boldsymbol{x}, \boldsymbol{x}_d)$ that satisfies, at least in a neighborhood of the stationary solution:

$$\boldsymbol{0} = \boldsymbol{g}(\boldsymbol{x}, \boldsymbol{x}_d, \boldsymbol{\rho}(\boldsymbol{x}, \boldsymbol{x}_d)) \tag{13}$$

Although the existence of the function $\boldsymbol{\rho}$ is guaranteed by the implicit function theorem, it is generally impossible to find explicitly such a function for practical systems. However, (9) provides the same asymptotic stability information for the original DDAE problem (5) as that of the theoretical DDE problem obtained by substituting the algebraic variable with the formal $\boldsymbol{\rho}$ function.

Equation (9) is a particular case of the standard form of the linear delay differential equations:

$$\dot{\boldsymbol{x}} = \boldsymbol{A}_0\boldsymbol{x}(t) + \sum_{i=1}^{\nu} \boldsymbol{A}_i\boldsymbol{x}(t-\tau_i) \tag{14}$$

where, in this case, $\nu = 2$, $\tau_1 = \tau$ and $\tau_2 = 2\tau$. The substitution of a sample solution of the form $e^{\lambda t}\boldsymbol{\upsilon}$, with $\boldsymbol{\upsilon}$ a non-trivial possibly complex vector of order n, leads to the *characteristic equation* of (14):

$$\det \Delta(\lambda) = 0 \tag{15}$$

where

$$\Delta(\lambda) = \lambda\boldsymbol{I}_n - \boldsymbol{A}_0 - \sum_{i=1}^{\nu} \boldsymbol{A}_i e^{-\lambda\tau_i} \tag{16}$$

is called the *characteristic matrix* [27]. In (16), $\boldsymbol{I}_n$ is the identity matrix of order n. The solutions of (16) are called the *characteristic roots* or *spectrum*, similar to the finite-dimensional case (i.e., the case for which $\boldsymbol{A}_i = \boldsymbol{0}$ $\forall i = 1, \ldots, \nu$). However, since (16) is transcendental, it has infinitely many roots, and thus one can only approximate the solution of (16) computing a reduced set of its roots.

Similar to the finite-dimensional case, the stability of (14) can be defined based on the sign of the roots of (16), i.e., the stationary point is stable if all roots have negative real part, and unstable if there exists at least one eigenvalue with positive real part.

Although the number of roots is infinite, there are two useful properties of the characteristic matrix that allows its exploitation for stability studies, as follows [27].

1) Equation (16) only has a finite number of characteristic roots in any vertical strip of the complex plane, given by $\{\lambda \in \mathbb{C} : \alpha < \Re(\lambda) < \beta\}$
2) There exists a number $\gamma \in \mathbb{R}$ such that all characteristic roots of (16) are confined to the half-plane $\{\lambda \in \mathbb{C} : \Re(\lambda) < \gamma\}$.

These properties basically imply that the number of solutions in the right-half of the complex plane is finite and, clearly, if $\gamma \leq 0$, there is no eigenvalue with positive real part. Thus, when one is only interested in the small-signal stability of the stationary solution of (5), the problem of finding the roots of (16) reduces to the problem of finding a finite number (possibly none) of roots of (16) with positive real part or poorly damped.

As briefly discussed in the Introduction, the idea to find an exact explicit solution of (16) has to be abandoned for practical systems. In this paper we use the technique proposed in [18]–[20] based on recasting (14) as an abstract Cauchy problem. This approach consists in transforming the original problem of computing the roots of a retarded functional differential

equations as a matrix eigenvalue problem of a PDE system of infinite dimensions and then approximating such system by means of a finite element method.

To better illustrate the method, let us assume some simplifications. First, assume that (5) has only one delay τ common to all retarded variables. Moreover, assume that $\boldsymbol{A}_2 = \boldsymbol{0}$. This hypothesis is actually a consequence of considering that in (5) only algebraic variables depend on the delay. Hence, (5) becomes:

$$\begin{aligned} \dot{\boldsymbol{x}} &= \boldsymbol{f}(\boldsymbol{x}, \boldsymbol{y}, \boldsymbol{y}_d, \boldsymbol{u}) \\ \boldsymbol{0} &= \boldsymbol{g}(\boldsymbol{x}, \boldsymbol{y}, \boldsymbol{u}) \end{aligned} \tag{17}$$

and from (11) and (12) one obtains:

$$\boldsymbol{A}_1 = -\boldsymbol{f}_{\boldsymbol{y}_d}\boldsymbol{g}_{\boldsymbol{y}}^{-1}\boldsymbol{g}_{\boldsymbol{x}}, \qquad \boldsymbol{A}_2 = \boldsymbol{0} \tag{18}$$

from which, (16) becomes:

$$\Delta(\lambda) = \lambda \boldsymbol{I}_n - \boldsymbol{A}_0 - \boldsymbol{A}_1 e^{-\lambda\tau} \tag{19}$$

Observe that the simplified index-1 Hessenberg form (17) is generally sufficient to describe electric power systems [8] and it is also the form used in the case study of this paper.

Then, one has to choose the numbers of nodes composing Chebyshev's discretization scheme, say N. This number affects the precision and the computational burden of the method, as it is explained below. Let $\boldsymbol{D}_N$ be Chebyshev's differentiation matrix of order N (see Appendix II) and define

$$\boldsymbol{M} = \left[\begin{array}{cccccc} \multicolumn{5}{c}{\hat{\boldsymbol{C}} \otimes \boldsymbol{I}_n} \\ \hline \boldsymbol{A}_1 & \boldsymbol{0} & & \dots & \boldsymbol{0} & \boldsymbol{A}_0 \end{array}\right] \tag{20}$$

where $\otimes$ indicate Kronecker's product (see Appendix III); $\boldsymbol{I}_n$ is the identity matrix of order n; and $\hat{\boldsymbol{C}}$ is a matrix composed of the first $N-1$ rows of $\boldsymbol{C}$ defined as follows:

$$\boldsymbol{C} = -2\boldsymbol{D}_N/\tau \tag{21}$$

Then, the eigenvalues of $\boldsymbol{M}$ are an approximated spectrum of (19).

Roughly speaking, one can see $\boldsymbol{M}$ as the discretization of a PDE system where the continuous variable, say ξ, corresponds to the time delay. Then ξ is discretized along a grid of N points. The position of such points are defined by Chebyshev's polynomial interpolation. The last n rows of $\boldsymbol{M}$ correspond to the PDE boundary conditions $\xi = \tau$ (e.g., $\boldsymbol{A}_1$) and $\xi = 0$ (e.g., $\boldsymbol{A}_0$), respectively. This suggests also how to generalize $\boldsymbol{M}$ for a case of characteristic equations with $\nu > 1$. For example, the matrix $\boldsymbol{M}$ for $\nu = 2$ can be formulated as follows:

$$\boldsymbol{M} = \left[\begin{array}{cccccc} \multicolumn{5}{c}{\hat{\boldsymbol{C}} \otimes \boldsymbol{I}_n} \\ \hline \boldsymbol{A}_2 & \boldsymbol{0}\dots\boldsymbol{0} & \boldsymbol{A}_1 & \boldsymbol{0}\dots\boldsymbol{0} & \boldsymbol{A}_0 \end{array}\right] \tag{22}$$

where $N+1$ must be odd to allow $\boldsymbol{A}_1$ being in the central node of Chebyshev's grid. As it can be expected, the general case with multiple delays can be assessed at the cost of increasing N and, hence, the size of the matrix $\boldsymbol{M}$, and of modifying accordingly its last n rows. The interested reader can find further insights on the multiple delay case in [20] and [28]. For the sake of simplicity, in this paper, only the case of a single delay is considered. This assumption is justified by the fact that the delays originate from an unique device type, e.g., the synchronous machine AVR, whose functioning has to be expected to be very similar, if not the same, for different machines.

B. Numerical Integration of Hessenberg DDAE of Retarded Type

Integrating general delay differential equations is not an easy task and specific methods have to be developed to avoid numerical instability. For example, despite being A-stable for standard DAE equations, the implicit trapezoidal method may shows numerical issues in case of DDAE. Thus, specific time integration methods for DDAE have been developed. We cite for example the two-stage Lobatto IIIC method [19].

Although the general case can show interesting numerical issues, in this paper we focus only on a subset of DDAE, namely the index-1 Hessenberg form (5). Furthermore, since most power system programs internally implement an implicit trapezoidal method for time domain integration, we provide the modifications that are required to adapt the implicit trapezoidal method to (5).

Let us define, for the sake of generality two general functional expressions:

$$\boldsymbol{0} = \boldsymbol{\phi}(\boldsymbol{x}, \boldsymbol{x}_d, t) = \hat{\boldsymbol{x}}(\boldsymbol{\alpha}(\boldsymbol{x}, t)) - \boldsymbol{x}_d \tag{23}$$

$$\boldsymbol{0} = \boldsymbol{\psi}(\boldsymbol{y}, \boldsymbol{y}_d, t) = \hat{\boldsymbol{y}}(\boldsymbol{\beta}(\boldsymbol{y}, t)) - \boldsymbol{y}_d \tag{24}$$

where $\boldsymbol{\alpha}(\boldsymbol{x}, t)$ and $\beta(\boldsymbol{y}, t)$ represent the functional dependence of state and algebraic variables on the delays. For the pure constant delays (2) and (3), one simply has:

$$\boldsymbol{\alpha}(\boldsymbol{x}, t) = t - \boldsymbol{\tau}, \qquad \boldsymbol{\beta}(\boldsymbol{y}, t) = t - \boldsymbol{\tau}\ , \tag{25}$$

but, of course, more complex expressions can be considered [19].

The implicit trapezoidal method for standard DAE (1) requires factorizing at each iteration i the Jacobian matrix [29]:

$$\boldsymbol{A}_c^{(i)} = \begin{bmatrix} \boldsymbol{I}_n - 0.5\Delta t \boldsymbol{f}_{\boldsymbol{x}}^{(i)} & -0.5\Delta t \boldsymbol{f}_{\boldsymbol{y}}^{(i)} \\ \boldsymbol{g}_{\boldsymbol{x}}^{(i)} & \boldsymbol{g}_{\boldsymbol{y}}^{(i)} \end{bmatrix} \tag{26}$$

where Δt is the time step at iteration i. Applying the same rule to (5) and using the functional equations (23) and (24), one obtains:

$$\boldsymbol{A}_c = \tag{27}$$
$$\begin{bmatrix} \boldsymbol{I}_n - 0.5\Delta t \boldsymbol{f}_{\boldsymbol{x}} & -0.5\Delta t \boldsymbol{f}_{\boldsymbol{y}} & -0.5\Delta t \boldsymbol{f}_{\boldsymbol{x}_d} & -0.5\Delta t \boldsymbol{f}_{\boldsymbol{y}_d} \\ \boldsymbol{g}_{\boldsymbol{x}} & \boldsymbol{g}_{\boldsymbol{y}} & \boldsymbol{g}_{\boldsymbol{x}_d} & \boldsymbol{0} \\ \boldsymbol{\phi}_{\boldsymbol{x}} & \boldsymbol{0} & \boldsymbol{\phi}_{\boldsymbol{x}_d} & \boldsymbol{0} \\ \boldsymbol{0} & \boldsymbol{\psi}_{\boldsymbol{y}} & \boldsymbol{0} & \boldsymbol{\psi}_{\boldsymbol{y}_d} \end{bmatrix}$$

where the superscript i has been omitted to simplify the notation. From (23) and (24), $\boldsymbol{\phi}_{\boldsymbol{x}_d} = -\boldsymbol{I}_{n_{xd}}$ and $\boldsymbol{\psi}_{\boldsymbol{y}_d} = -\boldsymbol{I}_{n_{yd}}$ are negative identity matrices, while $\boldsymbol{\phi}_{\boldsymbol{x}}$ and $\boldsymbol{\psi}_{\boldsymbol{y}}$ can be obtained by the chain rule:

$$\boldsymbol{\phi}_{\boldsymbol{x}} = \operatorname{diag}\left\{\dot{\hat{\boldsymbol{x}}}(\boldsymbol{x}, t)\right\} \boldsymbol{\alpha}_{\boldsymbol{x}} \tag{28}$$

$$\boldsymbol{\psi}_{\boldsymbol{y}} = \operatorname{diag}\left\{\dot{\hat{\boldsymbol{y}}}(\boldsymbol{y}, t)\right\} \boldsymbol{\beta}_{\boldsymbol{y}} \tag{29}$$

where $\dot{\hat{\boldsymbol{x}}}(\boldsymbol{x}, t)$ and $\dot{\hat{\boldsymbol{y}}}(\boldsymbol{y}, t)$ are the rate of change of $\boldsymbol{x}$ and $\boldsymbol{y}$ at time $\boldsymbol{\alpha}(\boldsymbol{x}, t)$ and $\boldsymbol{\beta}(\boldsymbol{y}, t)$, respectively, i.e., some time in

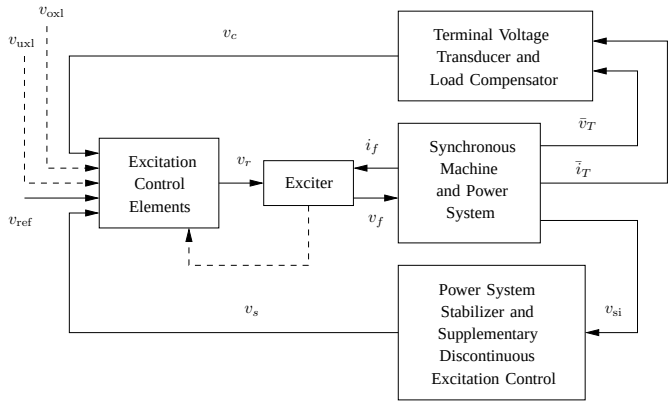

Fig. 1. General functional block diagram for synchronous machine excitation control system [30].

the past. While $\dot{\hat{\boldsymbol{x}}}(\boldsymbol{x},t)$ is easy to obtain by simply storing $\dot{\boldsymbol{x}}$ during the time domain integration, $\dot{\hat{\boldsymbol{y}}}(\boldsymbol{y},t)$ requires an extra computation, i.e., solving at each time t the following equation:

$$\mathbf{0} = \boldsymbol{g}_{\boldsymbol{x}}\boldsymbol{f} + \boldsymbol{g}_{\boldsymbol{y}}\dot{\boldsymbol{y}} + \boldsymbol{g}_{\boldsymbol{x}_d}\dot{\hat{\boldsymbol{x}}}\boldsymbol{\alpha}_t \tag{30}$$

from which $\dot{\boldsymbol{y}}$ can be obtained (if $\boldsymbol{g}_{\boldsymbol{y}}$ is not singular) and stored. Observe that $\dot{\boldsymbol{y}}$ can be discontinuous.

The simple structure of the Jacobian matrices of $\boldsymbol{\phi}$ and $\boldsymbol{\psi}$ allows rewriting (27) as (see Appendix IV):

$$\boldsymbol{A}_c = \begin{bmatrix} \boldsymbol{I}_n - 0.5\Delta t(\boldsymbol{f}_{\boldsymbol{x}} + \boldsymbol{f}_{\boldsymbol{x}_d}\boldsymbol{\phi}_{\boldsymbol{x}}) & -0.5\Delta t(\boldsymbol{f}_{\boldsymbol{y}} + \boldsymbol{f}_{\boldsymbol{y}_d}\boldsymbol{\psi}_{\boldsymbol{y}}) \\ \boldsymbol{g}_{\boldsymbol{x}} + \boldsymbol{g}_{\boldsymbol{x}_d}\boldsymbol{\phi}_{\boldsymbol{x}} & \boldsymbol{g}_{\boldsymbol{y}} \end{bmatrix} \tag{31}$$

Equation (31) is general and can be used for any kind of time-varying delay. In case of constant time delays, i.e., (2) and (3), it is straightforward to observe that $\boldsymbol{\alpha}_{\boldsymbol{x}} = \mathbf{0}$ and $\boldsymbol{\beta}_{\boldsymbol{y}} = \mathbf{0}$ and, hence, $\boldsymbol{\phi}_{\boldsymbol{x}} = \mathbf{0}$ and $\boldsymbol{\psi}_{\boldsymbol{y}} = \mathbf{0}$. Hence, for pure constant delays, (26) and (31) coincide. This results was to be expected since at a given time t, both $\boldsymbol{x}_d$ and $\boldsymbol{y}_d$, i.e., state and algebraic variables delayed by τ, are constants.

III. Modeling the Synchronous Machine Excitation Control System

The general functional block of a synchronous machine excitation system is depicted in Fig. 1. The main signals required by the excitation system are the voltage signal v_c, the field voltage v_f and current i_f, the reference voltage $v_{\rm ref}$ and additional inputs, such as the power system stabilizer signal v_s and the over- and under-excitation signals, $v_{\rm oxl}$ and $v_{\rm uxl}$, respectively.

The voltage signal v_c is a function of the synchronous machine terminal voltage $\bar{v}_T$ and current $\bar{i}_T$ if the load compensation is used and of the transducer dynamics, as follows:

$$\begin{aligned} v_c' &= |\bar{v}_T \pm (r_c + jx_c)\bar{i}_T| && (32)\\ \dot{v}_c &= (v_c' - v_c)/T_r && (33) \end{aligned}$$

where r_c and x_c are the load compensation resistance and reactance, respectively, and T_r is a time constant that take into account the transducer low pass filter and delay [31].

The excitation control system output signal v_r depends on the AVR type. For static exciters, v_r is a voltage signal that is processed through transducers and gate pulse generators to properly control the thyristor bridge that feeds the field winding of the generator. Finally, the excitation control system typically consists of digital hardware [32], [33] or, in most recent systems, of a programmable logic controller (PLC) [34].

In the common practice, pure delays introduced by the transducers and the control digital system are neglected. Most of these delays are negligible indeed. For example digital amplifiers and analog-to-digital converters have delays of the order of 10 μs, while anti-aliasing-filters have a delay of about 70 μs and decimation stages of about 225 μs [35]. However, the PLC executes the AVR algorithms and other AVR secondary functions within a 3 to 15 ms period [34]. If the voltage controlled by the AVR is on a remote bus, measurement delays can drastically increase, i.e., more than 100 ms [7].

In this paper, we propose to take into account the delays introduced by the excitation control system by including an overall delay in the output signal v_c' of the terminal (or remote) voltage transducer. Thus, equation (33) becomes:

$$\dot{v}_c = (v_c'(t-\tau_v) - v_c)/T_r \tag{34}$$

If, for simplicity, but without loss of generality, load compensation is not used, the delay affects directly the synchronous machine terminal voltage, and (32)-(33) become:

$$\dot{v}_c = (v_T(t-\tau_v) - v_c)/T_r \tag{35}$$

Similarly to AVR delays (34) or (35), we also consider delays in the measures of the PSS v_s similarly to the work that was done in [7]. Also in this case, local measures have at most a few ms delay while remote measures can be affected by a delay of up to 100 ms or more [7]. In typical PSSs, the signal $v_{\rm si}$ is the synchronous machine rotor speed ω, which is a state variable. Hence, in this case, one has $x_d = \omega(t-\tau_\omega)$. Moreover, a typical PSS control scheme include a washout filter and two lead-lag blocks (see Fig. 2). Thus the retarded measure of ω propagates in the PSS equations, as follows:

$$\begin{aligned} \dot{v}_1 &= -(K_w\omega(t-\tau_\omega) + v_1)/T_w && (36)\\ \dot{v}_2 &= ((1-\frac{T_1}{T_2})(K_w\omega(t-\tau_\omega) + v_1) - v_2)/T_2 \\ \dot{v}_3 &= ((1-\frac{T_3}{T_4})(v_2 + (\frac{T_1}{T_2}(K_w\omega(t-\tau_\omega) + v_1))) - v_3)/T_4 \\ 0 &= v_3 + \frac{T_3}{T_4}(v_2 + \frac{T_1}{T_2}(K_w\omega(t-\tau_\omega) + v_1)) - v_s \end{aligned}$$

where v_1, v_2 and v_3 are state variables introduced by the PSS washout filter and by lag blocks and other parameters are illustrated in Fig. 2. Observe that equations (36) are in the form of (5) with $\boldsymbol{x} = (v_1, v_2, v_3)$, $\boldsymbol{x}_d = \omega(t-\tau_\omega)$, and $\boldsymbol{y} = v_s$.

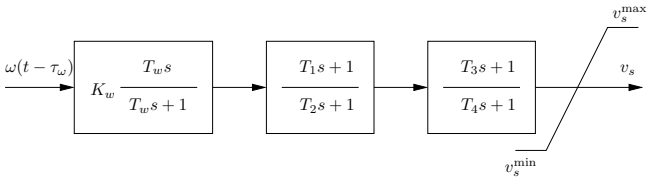

Fig. 2. Power system stabilizer control diagram [29].

IV. Case Study

There are at least two possible ways of approaching the study of bifurcation points and, hence, the small-signal stability, of a retarded system.

1) To define the maximum delay τ that drives the system to the frontier of the stability region. This is basically the *delay margin* definition given in [11]. This definition makes sense if the delay is an independent variable and there is only one delay to deal with. In this case, the delay can be viewed as a bifurcation parameter similarly to the loading parameter in voltage stability studies [36].
2) To define the properties of the equilibria of the retarded system. Delays are given as the functionals (23) and (24). In this case, delays are system variables, i.e., $\boldsymbol{x}_d$ and $\boldsymbol{y}_d$ in (5), of any order, while the bifurcation parameter can be, for example, a scalar loading factor μ that multiplies load power consumptions as in voltage and small-signal angle stability studies [36] and [37].

Both analyses are considered in this paper, however, we consider that the second approach is the one with most practical interest. In particular, Subsection IV-B describes the bifurcation analysis as well as the power system model used to define the loading margin for the DDAE and IV-C depicts and discusses some relevant time domain simulation results.

The systems considered in this paper are the IEEE 14-bus system and a real world 1213-bus system, as follows.

1) The IEEE 14-bus system consists of two generators, three synchronous compensators, two two-winding and one three-winding transformers, fifteen transmission lines, eleven loads and one shunt capacitor (see Fig. 3). Not depicted in Fig. 3, but included in the system model, are generator controllers, such as the primary voltage regulators. All dynamic data of this system as well as a detailed discussion of its transient behavior can be found in [29].
2) The real-world transmission system contains 1213 buses, 973 transmission lines, 718 transformers and 113 synchronous generators. The dynamic order of this system is $n = 753$. The AVRs of all synchronous machines have a measurement delay τ_v. The aim of this case study is to show the robustness and the computational burden of the proposed technique.

The AVR control scheme of the dc exciter model used in this case study and is a simplified version of the classic IEEE type DC1 that is defined in [30] and fully described in [29]. The standard IEEE type DC1 model does not include time delays.

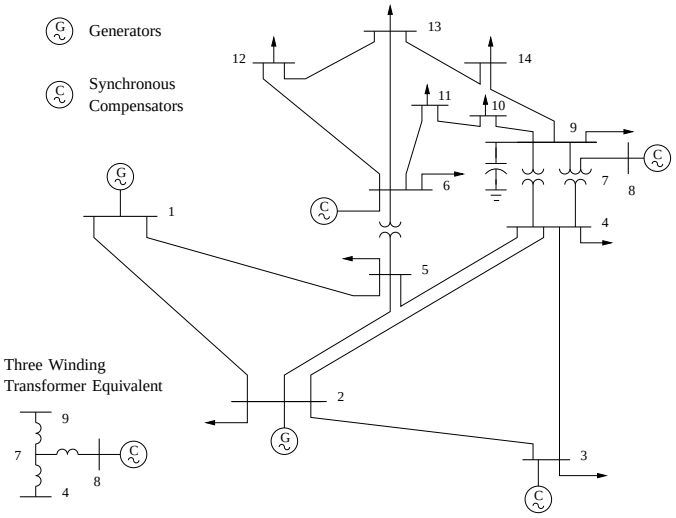

Fig. 3. IEEE 14-bus test system.

All simulations and plots are obtained using a novel Python-based version of PSAT [38]. This PSAT version requires Python 2.7.1 (`http://www.python.org`), Numpy 1.5.1 (`http://numpy.scipy.org`), CVXOPT 1.1.3 (`http://abel.ee.ucla.edu/cvxopt/`), and Matplotlib 1.0.0 (`http://matplotlib.sourceforge.net/`) and has been executed on a 64 bit Linux Fedora Core 14 platform running on a 1.73 GHz Intel Core i7 with 8 GB of RAM.

A. Computational Burden of the Spectrum Evaluation

Before entering into the details of the stability analysis of the DDAE, it is worthwhile to discuss the computational burden of the proposed technique for evaluating an approximated solution of (16). With this aim, Table I shows the computational burden of the spectrum analysis for the IEEE 14-bus system for $\tau_v = 5$ ms and for different values of N. Table I also shows the computational burden of the standard eigenvalue analysis (i.e., no delays) that consists in solving

$$\Delta(\lambda) = \boldsymbol{I}_n \lambda - \boldsymbol{A}_s \tag{37}$$

where $\boldsymbol{A}_s$ is the state matrix of the DAE system obtained neglecting time delays in the AVR model. This case is indicated as $N = 1$ in Table I. Moreover, NNZ indicates the number of non-zero elements of matrix $\boldsymbol{M}$. The size of $\boldsymbol{M}$ is $N \cdot n$, where n is the dynamic order of the system (in this example, $n = 49$). Observe that the matrix $\boldsymbol{M}$ is highly sparse and its sparsity increases as N increases. CPU times given in Table I refers to the computation of all eigenvalues of $\boldsymbol{M}$. Clearly, the higher N, the higher the CPU time.

Figure 4 shows the root loci of $\boldsymbol{M}$ for the IEEE 14-bus system for different values of N. Most eigenvalues have a very high frequency. Actually, only a very reduced number of eigenvalues is interesting for small-signal stability analysis, i.e., those that have positive real part or that are closer to the imaginary axis. This fact allows using some efficient technique for determining only a reduced number of eigenvalues of

TABLE I

COMPUTATIONAL BURDEN OF THE SPECTRUM ANALYSIS FOR $\tau_v = 5$ ms AND FOR THE IEEE 14-BUS SYSTEM FOR DIFFERENT VALUES OF N

N	CPU time (s)	$N \cdot n$	$(N \cdot n)^2$	NNZ	NNZ$/(N \cdot n)^2$
1	0.031	49	2 401	776	32.3%
5	0.065	245	59 049	1 707	2.83%
10	0.223	490	240 100	5 186	2.15%
20	1.609	980	960 400	19 396	2.02%
40	9.392	1 960	3 841 600	77 216	2.01%

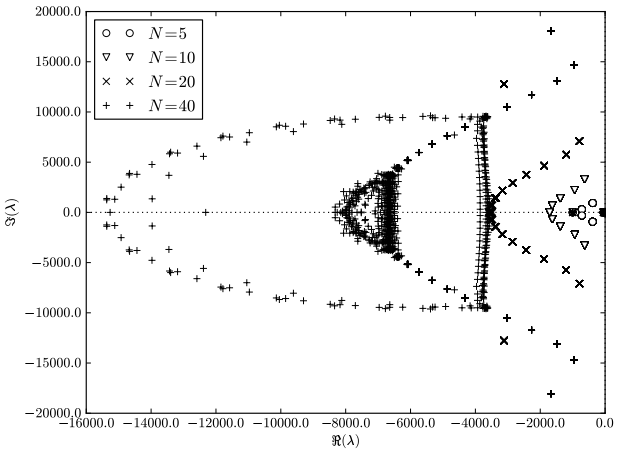

Fig. 4. Root loci of the IEEE 14-bus system modeled as a DDAE for $\tau_v = 5$ ms and for different values of N.

$\boldsymbol{M}$ (e.g., Rayleigh's iteration, Arnoldi's iteration, etc.). The interested reader can see a description of efficient iterative methods for determining a reduced number of eigenvalues in [29].

Figure 5 shows a zoom of the eigenvalue loci depicted in Fig. 4. It is interesting to observe that the eigenvalues of $\boldsymbol{M}$ closest to the imaginary axis are not sensible to N. The values shown in Fig. 5 vary less than 10^{-6} when N varies from 5 to 40. From the computational viewpoint, this is an important advantage of the proposed method for computing the spectrum of (16). Since the sensitivity of the rightmost real part eigenvalues is small with respect to N, one can keep N relatively small and, hence, reduce the computational burden while evaluating the spectrum of (16).

The fact that the sensitivity of the rightmost eigenvalues of $\boldsymbol{M}$ is small with respect to N is discussed in mathematical terms in [18]–[20]. Here, we provide only an intuitive justification, as follows. The solution of (19) has n eigenvalues "close" to the eigenvalues of $\boldsymbol{A}_0$ (as a matter of fact, if the delays are zero, the DDAE becomes a DAE), and an infinite number of other eigenvalues with higher frequency that the first n ones. Increasing N allows finding such higher frequency eigenvalues while little affecting eigenvalues with small magnitude.

From observing Fig. 5, only two complex eigenvalues appears to be critical, since have a damping ratio lower than 5%.[1]

[1]The zero eigenvalue shown in Figs. 4 and 5 is due to the arbitrariness of the synchronous angle reference and, hence, does not indicate a bifurcation.

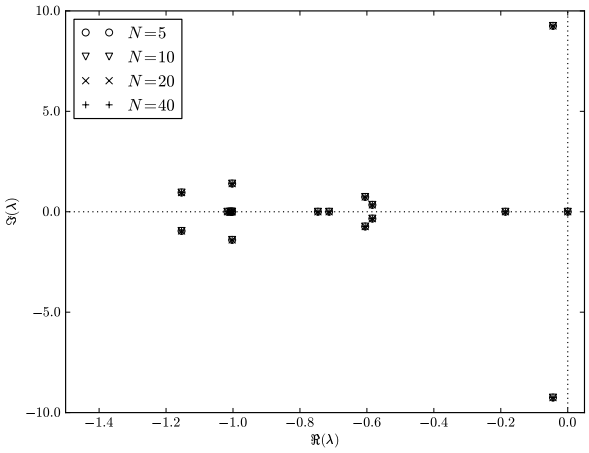

Fig. 5. Zoom close to the imaginary axis of the root loci of the IEEE 14-bus system modeled as a DDAE for $\tau_v = 5$ ms and for different values of N.

The fact that among all eigenvalues only very few are critical is a quite general result that applies for the majority of power systems. Thus, a possible efficient strategy for computing the critical eigenvalues of a DDAE system is as follows:

1) Compute the eigenvalues of the state matrix of order n of the system without considering delays. This is a standard eigenvalue analysis of a DAE system.
2) The critical eigenvalues and the associated eigenvectors obtained in the previous point can be used as initial guess for starting an iterative and efficient method such as the Rayleigh's iteration over the matrix $\boldsymbol{M}$.

According to this technique, the eigenvalue analysis of the DDAE system reduces to a standard eigenvalue analysis plus a certain number of matrix multiplications which have small computational burden compared to complete eigenvalue analysis of the full matrix $\boldsymbol{M}$. Applying such technique to the IEEE-14 bus system, we obtained a CPU times of about 0.67 s for determining the 50 eigenvalues with rightmost real part for the case with $N = 40$. It has to be expected that the higher the dynamic order n of the system, the higher the time saving. This statement is further discussed in the Subsection IV-D that presents a real-world case study.

B. Bifurcation Analysis

In this subsection, we consider the bifurcation analysis for the IEEE 14-bus system using two different bifurcation parameters: (i) the time delay τ_v; and (ii) the loading level of the system. While the first approach was proposed in [11], the latter technique is the most common bifurcation analysis that leads to obtain the well-known nose curves [36].

1) Using the time delay as the bifurcation parameter: The simulation presented in this section are aimed to define whether the inclusion of delays in the AVR equations of the IEEE 14-bus system can be approximated using the standard DAE model. We consider two cases: (i) equations (35), and (ii) a modified version of (33) in which the delay is summed

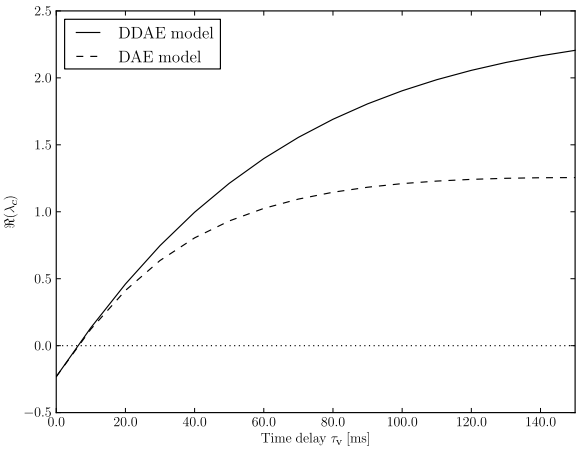

Fig. 6. Real part of the critical eigenvalue λ_c of the IEEE 14-bus system as a function of the AVR voltage measure time delay τ_v.

to the filter time constant T_r:

$$\dot{v}_c = (v_T - v_c)/(T_r + \tau_v) \tag{38}$$

For similarity with (35), but without lack of generality, no load compensation is considered in (38). In both cases, $T_r = 0.001$ s is used.

Figure 6 shows the real part of the critical eigenvalue λ_c of the IEEE 14-bus system as a function of the AVR voltage measure time delay τ_v, which is varied in the interval $[0, 150]$ ms. For $\tau_v < 15$ ms, the difference between the DAE and the DDAE models is negligible. This result actually confirms the common practice of neglecting constant delays for local measures of terminal voltage. However, as the delay increases, the difference between the DAE and DDAE system is quite evident. This justifies the use of the DDAE model in case of remote measures of bus voltages used as input signals of the AVR system.

The Hopf bifurcation (HB) occurs for $\tau_v \approx 6.3$ ms, which is thus the *delay margin* of the AVRs. In this case the HB occurs in a region for which the DAE and the DDAE models behave similarly. Thus, there is no clear advantage of using the DDAE model in this case. The usefulness of the DDAE model is better shown in Subsection IV-C that concerns the behavior of the PSS with remote measures.

Observe that $\lim \Re(\lambda_c)$ for $\tau_v \to 0$ is the same for both the DAE and the DDAE models. In fact, as $\tau \to 0$, (16) degenerates as:

$$\lim_{\tau \to 0} \Delta(\lambda) = \boldsymbol{I}_n \lambda - (\boldsymbol{A}_0 + \boldsymbol{A}_1) = \boldsymbol{I}_n \lambda - \boldsymbol{A}_s \tag{39}$$

The fact that $\boldsymbol{A}_0 + \boldsymbol{A}_1 \to \boldsymbol{A}_s$ as $\tau \to 0$ can be seen in two ways, as follows.

1) As $\tau \to 0$, $\boldsymbol{y}_d$ and $\boldsymbol{x}_d$ degenerate into non-delayed variables $\boldsymbol{y}$ and $\boldsymbol{x}$, respectively, hence $\boldsymbol{A}_1$ has to be merged into $\boldsymbol{A}_0$
2) If $\tau = 0$, $\boldsymbol{y}_d = \boldsymbol{x}_d = \boldsymbol{0}$ and $\boldsymbol{A}_1 = \boldsymbol{0}$, whereas $\boldsymbol{A}_0$ has to be recast and $\boldsymbol{A}_0 = \boldsymbol{A}_s$.

TABLE II

LOADING LEVELS $\mu_{\rm HB}$ CORRESPONDING TO THE OCCURRENCE OF HB FOR THE IEEE 14-BUS SYSTEM FOR DIFFERENT VALUES OF τ_v

τ_v [ms]	$\mu_{\rm HB}$ [pu]	$\Delta\mu$ [%]
0	1.202	-
1	1.175	2.24
5	1.048	12.8
10	0.805	33.0

In any case, (39) must hold. Observe also that $\boldsymbol{M}$ cannot be computed for $\tau = 0$ due to the definition of $\boldsymbol{C}$ in (21).

2) Using the loading level as the bifurcation parameter: In this case, we use a scalar variable, say μ, to parameterize the loading level of the overall system, as follows [29]:

$$\begin{aligned} \boldsymbol{p}_G &= (\mu \boldsymbol{I}_{n_G} + k_G \boldsymbol{\Gamma}) \boldsymbol{p}_{G0} \\ \boldsymbol{p}_L &= \mu \boldsymbol{p}_{L0} \\ \boldsymbol{q}_L &= \mu \boldsymbol{q}_{L0} \end{aligned} \tag{40}$$

where $\boldsymbol{I}_{n_G}$ is the identity matrix of order n_G, being n_G the number of generators, $\boldsymbol{\Gamma} = \text{diag}(\gamma_1, \gamma_2, \ldots, \gamma_{n_G})$ are generator loss participation factors, k_G is a scalar variable used for accomplishing the distributed slack bus model as discussed in [29] and $\boldsymbol{p}_{G0}$, $\boldsymbol{p}_{L0}$ and $\boldsymbol{q}_{L0}$ are the "base case" or initial generator and load powers, respectively. This is the common model used in continuation power flow studies [36]. For each value of μ a power flow solution is found and the equilibrium of the DAE system is computed.

An HB occurs for $\mu \approx 1.202$ if considering the standard DAE model and no contingencies [29]. Table II shows the values of the loading level μ for which a HB occurs for different values of τ_v. As it was to be expected from the discussion in the previous section, as τ_v increases, the HB occurs for lower values of μ. Observe that for $\tau_v = 10$ ms, $\mu_{\rm HB} < 1$, which means that the base case operating condition is not stable. Similar tables can be obtained considering contingencies, which are not included in the paper for the sake of space. The results of Table II can be viewed in two different ways:

1) The effect of time delays is actually that of reducing the loading margin of the system. This is the direct information given in Table II.
2) The effect of time delays can be interpreted as a "virtual" load increase. For example, $\tau_v = 5$ ms is equivalent to a load increase of 12.8%.

In any case, there is a clear interest in reducing as much as possible control time delays.

C. Time Domain Simulation Results

In this subsection, we illustrate through time domain simulations the effect of the time delay in the measure of synchronous machine rotor speed when used as input signal for the PSS device. From [29], it is known that the IEEE 14-bus system is prone to show an HB if increasing the loading level by 20% with respect to the base case and applying a line 2-4 outage. The HB can be removed by including the PSS of Fig. 2 in the excitation control scheme of the machine connected to bus 1.

For the sake of example, we assume that such PSS is affected by a delay τ_ω in the measure of ω. Furthermore, to force instability, we also assume that the measure of ω is remote. This hypothesis can be justified by observing that the machine at bus 1 is actually an equivalent model of a bigger network (in fact the IEEE 14-bus system is obtained by simplifying the IEEE 30-bus system). Thus, if we assume that such equivalent network includes an SPSS as described in [7], we can consider a delay of tens of milliseconds in the measure of ω (e.g., 100 ms delay is used in [7]). In the following example, we only consider the delay in the PSS model and no delays in the AVR measures.

By repeating the analysis of the delay margin, we obtain that for a 20% increase of the loading level with respect of the base case and for line 2-4 outage, a HB occurs for $\tau_\omega \approx 68.6$ ms. However, without the line outage, the HB occurs for $\tau_\omega > 72$ ms. Thus, setting $72 > \tau_\omega > 69$ ms, it has to be expected that the transient following line 2-4 outage is unstable, while the initial equilibrium point without contingency is stable, though poorly damped.

Figure 7 shows the time response of the IEEE 14-bus system without PSS, with PSS and with retarded PSS with $\tau_\omega = 71$ ms. As already known from [29], the trajectory of the system without PSS enters into a limit cycle after the line outage while the system with PSS is asymptotically stable. The behavior of the system with retarded PSS is similar to the case without PSS, i.e., shows a limit cycle trajectory. This results was to be expected, since if $\tau_\omega \to \infty$, the PSS control loop opens and the effect is the same as the system without PSS. However, the small-signal stability is able to determine the exact value for which the HB occurs. The added value of the time domain simulation is to show that the system trajectory enters into a limit cycle rather than diverging.

The HB shown Fig. 7 is almost certainly super-critical since it ends up in a stable limit cycle. In our experience, power system can show both super- and sub-critical HBs. A famous example of sub-critical HB is the one that led to the 1996 WSCC blackout. However, regardless their type, HBs have always to be avoided in power system operation. In fact, sub-critical HBs likely lead to a system collapse, whereas super-critical ones lead to loss increase, inter-area power oscillations and, possibly to untimely intervention of the protections that may cause dangerous cascading phenomena.

It has to be noted that, for finite-dimensional power system models (as in the case of standard DAE), HBs, which are co-dimension one local bifurcations, are *generic*. In other words, HBs are expected to occur given certain loading conditions and synchronous machine controllers. However, the case of infinite-dimensional dynamics such as delay systems requires further analysis to conclude on the genericity of the bifurcation points. This is currently an open field of research.

D. Real-world transmission system

Table III shows the computational burden for the 1213-bus system as a function of N. $N = 1$ indicates the standard eigenvalue analysis (i.e., no delays) and is included in Table III for the sake of comparison. As N increases, the computational burden grows quickly and highly nonlinearly, as it was to be expected. For the sake of illustration, Figs. 8 and 9 depict the root loci for $N = 20$.

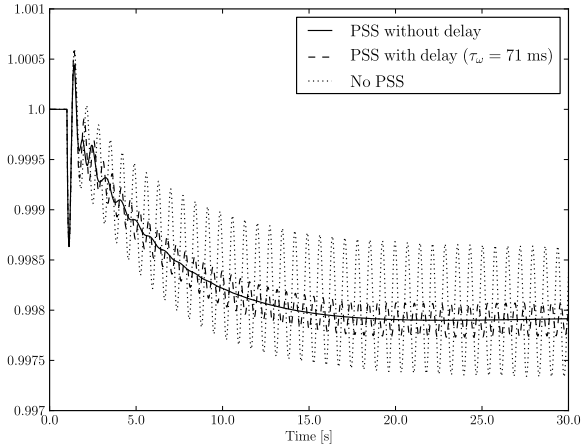

Fig. 7. Rotor speed ω of machine 5 for the IEEE 14-bus system with a 20% load increase and for different control models following line 2-4 outage at $t = 1$ s.

TABLE III
COMPUTATIONAL BURDEN OF THE SPECTRUM ANALYSIS FOR $\tau_v = 10$ ms AND FOR THE 1213-BUS SYSTEM FOR DIFFERENT VALUES OF N

N	Method	$N \cdot n$	CPU time
1	All	753	0.692 s
5	All	3 675	47.3 s
10	All	7 530	7 m 43 s
20	All	15 060	51 m 40 s
5	50 RM	3 675	0.573 s
10	50 RM	7 530	1.24 s
20	50 RM	15 060	2.19 s

As discussed above, computing all eigenvalues is not actually needed to assess small-signal stability, since only positive eigenvalues or those that are closer to the imaginary axis are of interest. In Table III, the computational burden of the full eigenvalue analysis as obtained using the QR decomposition is compared with that of a reduced eigenvalue analysis based on the Arnoldi's iteration. The QR decomposition and the Arnoldi's iteration are obtained linking Python to the LAPACK [39] and the ARPACK [40] libraries, respectively. As expected, computing a reduced set of eigenvalues and taking advantage of the sparsity of matrix $\boldsymbol{M}$ allows drastically reducing the CPU time. In Table III "50 RM" indicates that only the 50 rightmost eigenvalues have been computed.

Figure 10 shows that, as in the case of the IEEE 14-bus system, the sensitivity of the eigenvalues closer to the imaginary axis with respect to N is small. This property is quite important since it allows keeping a reduced size of $\boldsymbol{M}$ even for large systems. Observe that, in this real-world case study, the number of roots close to the imaginary axis and with poor damping is relatively high. This is due to two facts, as follows.

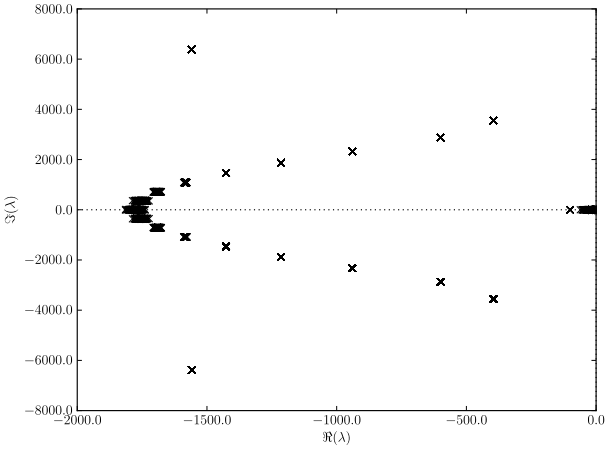

Fig. 8. Full root loci of the 1213-bus system for $\tau_v = 10$ ms and for $N = 20$.

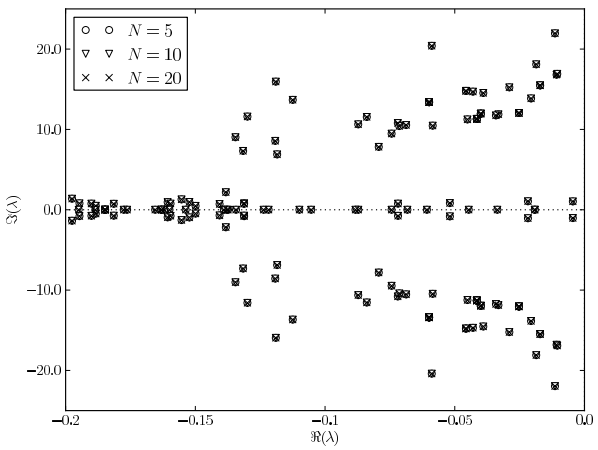

Fig. 10. Zoom close to the imaginary axis of the root loci of the 1213-bus system for $\tau_v = 10$ ms and for different values of N.

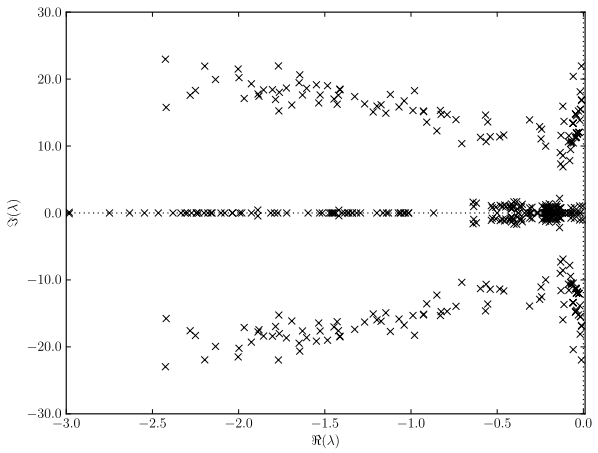

Fig. 9. Zoom close to the imaginary axis of the root loci of the 1213-bus system for $\tau_v = 10$ ms and for $N = 20$.

1) The system contains a high number of machines and AVRs, so even if the number of critical eigenvalues is a small percentage of the dynamic order n, the absolute number of poorly damped eigenvalues is relatively high.
2) Available data do not include PSSs, which would be certainly able to move several eigenvalues to the left of the complex plane.

The delay stability margin of the 1213-bus system can be computed in a similar way as discussed for the IEEE 14-bus system. In particular, a HB occurs for $\tau_v \approx 18.2$ ms.

V. Conclusions

This paper presents a relatively simple, yet efficacious method to define the small-signal stability of power systems modeled as DDAE. In particular, the index-1 Hessenberg form appears to be adequate for modeling the behavior of power systems when delays are taken into account. The proposed technique allows estimating an approximate solution of the characteristic equation of DDAE based on the Chebyshev's differentiation matrix.

The advantage of the method is that it is able to precisely estimate the rightmost eigenvalues while maintaining a tractable computational burden. The proposed technique is then applied to evaluate the delay margin as well as the effect of delays on the loading margin of the IEEE 14-bus test system and of a real-world 1213-bus system. AVR as well as PSS measure delays are considered and the results of small-signal stability analysis are confirmed by time domain simulations.

The main conclusion of this papers is that it is important to properly model time delays since these considerably affect the behavior of the overall power system, especially if considering remote measures. Thus, the applications of the proposed method are mainly in preventive control and dynamic security assessment of power systems. In particular, the estimation of the delay security margin can be used to accurately define the available transfer capability as defined by NERC [41].

The work presented in the paper suggests some interesting future research directions, such as considering multiple as well as time-varying time delays especially in the field of wide-area measurement systems and PMU devices. A detailed research on the generic bifurcations that may occur in power systems modelled as DDAE also appears as a challenging theoretical research field.

VI. Acknowledgments

The first author would like to thank Dr. Luigi Vanfretti, from KTH, Sweden, for the interesting discussion about AVR schemes.

Appendix I
Determination of $\boldsymbol{A}_0$, $\boldsymbol{A}_1$ and $\boldsymbol{A}_2$

This Appendix describes how (10)-(12) are determined based on (7)-(8). From (8), one obtains:

$$\Delta \boldsymbol{y} = -\boldsymbol{g}_{\boldsymbol{y}}^{-1}\boldsymbol{g}_{\boldsymbol{x}}\Delta \boldsymbol{x} - \boldsymbol{g}_{\boldsymbol{y}}^{-1}\boldsymbol{g}_{\boldsymbol{x}_d}\Delta \boldsymbol{x}_d \tag{41}$$

Substituting (41) into (7) one has:

$$\begin{aligned}\Delta\dot{\boldsymbol{x}} &= (\boldsymbol{f}_{\boldsymbol{x}} - \boldsymbol{f}_{\boldsymbol{y}}\boldsymbol{g}_{\boldsymbol{y}}^{-1}\boldsymbol{g}_{\boldsymbol{x}})\Delta\boldsymbol{x} + \\ &\quad (\boldsymbol{f}_{\boldsymbol{x}_d} - \boldsymbol{f}_{\boldsymbol{y}}\boldsymbol{g}_{\boldsymbol{y}}^{-1}\boldsymbol{g}_{\boldsymbol{x}_d})\Delta\boldsymbol{x}_d + \\ &\quad \boldsymbol{f}_{\boldsymbol{y}_d}\Delta\boldsymbol{y}_d\end{aligned} \tag{42}$$

In (42), one has still to substitute $\Delta\boldsymbol{y}_d$ for a linear expression of the actual and/or of the retarded state variable. With this aim, consider the algebraic equations $\boldsymbol{g}$ computed at $(t-\tau)$. Since algebraic constraints have always to be satisfied, the following steady-state condition must hold:

$$\boldsymbol{0} = \boldsymbol{g}(\boldsymbol{x}(t-\tau), \boldsymbol{x}_d(t-\tau), \boldsymbol{y}(t-\tau)) \tag{43}$$

Then, observing that $\boldsymbol{x}_d = \boldsymbol{x}(t-\tau)$, $\boldsymbol{y}_d = \boldsymbol{y}(t-\tau)$, and $\boldsymbol{x}_d(t-\tau) = \boldsymbol{x}(t-2\tau)$, differentiating (43) leads to:

$$\boldsymbol{0} = \boldsymbol{g}_{\boldsymbol{x}}\Delta\boldsymbol{x}_d + \boldsymbol{g}_{\boldsymbol{x}_d}\Delta\boldsymbol{x}(t-2\tau) + \boldsymbol{g}_{\boldsymbol{y}}\Delta\boldsymbol{y}_d \tag{44}$$

In steady-state, for any instant t_0, $\boldsymbol{x}(t_0) = \boldsymbol{x}(t_0-\tau) = \boldsymbol{x}(t_0-2\tau) = \boldsymbol{x}_0$ and $\boldsymbol{y}(t_0) = \boldsymbol{y}_d(t_0) = \boldsymbol{y}_0$. Hence, the Jacobian matrices in (44) are the same as in (8). Equation (44) can be rewritten as:

$$\Delta\boldsymbol{y}_d = -\boldsymbol{g}_{\boldsymbol{y}}^{-1}\boldsymbol{g}_{\boldsymbol{x}}\Delta\boldsymbol{x}_d - \boldsymbol{g}_{\boldsymbol{y}}^{-1}\boldsymbol{g}_{\boldsymbol{x}_d}\Delta\boldsymbol{x}(t-2\tau) \tag{45}$$

and, substituting (45) into (42), one obtains:

$$\begin{aligned}\Delta\dot{\boldsymbol{x}} &= (\boldsymbol{f}_{\boldsymbol{x}} - \boldsymbol{f}_{\boldsymbol{y}}\boldsymbol{g}_{\boldsymbol{y}}^{-1}\boldsymbol{g}_{\boldsymbol{x}})\Delta\boldsymbol{x} + \\ &\quad (\boldsymbol{f}_{\boldsymbol{x}_d} - \boldsymbol{f}_{\boldsymbol{y}}\boldsymbol{g}_{\boldsymbol{y}}^{-1}\boldsymbol{g}_{\boldsymbol{x}_d} - \boldsymbol{f}_{\boldsymbol{y}_d}\boldsymbol{g}_{\boldsymbol{y}}^{-1}\boldsymbol{g}_{\boldsymbol{x}})\Delta\boldsymbol{x}_d + \\ &\quad (-\boldsymbol{f}_{\boldsymbol{y}_d}\boldsymbol{g}_{\boldsymbol{y}}^{-1}\boldsymbol{g}_{\boldsymbol{x}_d})\Delta\boldsymbol{x}(t-2\tau)\end{aligned} \tag{46}$$

which leads to the definitions of $\boldsymbol{A}_0$, $\boldsymbol{A}_1$ and $\boldsymbol{A}_2$ given in (10), (11) and (12), respectively.

APPENDIX II
CHEBYSHEV'S DIFFERENTIATION MATRIX

Chebyshev's differentiation matrix $\boldsymbol{D}_N$ of dimensions $N+1 \times N+1$ is defined as follows. Firstly, one has to define $N+1$ Chebyshev's nodes, i.e., the interpolation points on the normalized interval $[-1, 1]$:

$$x_k = \cos\left(\frac{k\pi}{N}\right), \quad k = 0, \ldots, N. \tag{47}$$

Then, the element (i,j) differentiation matrix $\boldsymbol{D}_N$ indexed from 0 to N is defined as [42]:

$$\boldsymbol{D}_{(i,j)} = \begin{cases} \frac{c_i(-1)^{i+j}}{c_j(x_i - x_j)}, & i \neq j \\ -\frac{1}{2}\frac{x_i}{1-x_i^2}, & i = j \neq 1, N-1 \\ \frac{2N^2+1}{6}, & i = j = 0 \\ -\frac{2N^2+1}{6}, & i = j = N \end{cases} \tag{48}$$

where $c_0 = c_N = 2$ and $c_2 = \cdots = c_{N-1} = 1$. For example, $\boldsymbol{D}_1$ and $\boldsymbol{D}_2$ are:

$$\boldsymbol{D}_1 = \begin{bmatrix} \frac{1}{2} & -\frac{1}{2} \\ \frac{1}{2} & -\frac{1}{2} \end{bmatrix}, \quad \text{with } x_0 = 1,\ x_1 = -1\ .$$

and

$$\boldsymbol{D}_2 = \begin{bmatrix} \frac{3}{2} & -2 & \frac{1}{2} \\ \frac{1}{2} & 0 & -\frac{1}{2} \\ -\frac{1}{2} & 2 & -\frac{3}{2} \end{bmatrix}, \text{ with } x_0 = 1,\ x_1 = 0,\ x_2 = -1\ .$$

APPENDIX III
KRONECKER'S PRODUCT

If $\boldsymbol{A}$ is a $m \times n$ matrix and $\boldsymbol{B}$ is a $p \times q$ matrix, then Kronecker's product $\boldsymbol{A} \otimes \boldsymbol{B}$ is an $mp \times nq$ block matrix [43], as follows:

$$\boldsymbol{A} \otimes \boldsymbol{B} = \begin{bmatrix} a_{11}\boldsymbol{B} & \cdots & a_{1n}\boldsymbol{B} \\ \vdots & \ddots & \vdots \\ a_{m1}\boldsymbol{B} & \cdots & a_{mn}\boldsymbol{B} \end{bmatrix} \tag{49}$$

For example, let $\boldsymbol{A} = \begin{bmatrix} 1 & 2 & 3 \\ 3 & 2 & 1 \end{bmatrix}$ and $\boldsymbol{B} = \begin{bmatrix} 2 & 1 \\ 2 & 3 \end{bmatrix}$. Then:

$$\boldsymbol{A} \otimes \boldsymbol{B} = \begin{bmatrix} \boldsymbol{B} & 2\boldsymbol{B} & 3\boldsymbol{B} \\ 2\boldsymbol{B} & 2\boldsymbol{B} & \boldsymbol{B} \end{bmatrix} = \begin{bmatrix} 2 & 1 & 4 & 2 & 6 & 3 \\ 2 & 3 & 4 & 6 & 6 & 9 \\ 6 & 3 & 4 & 2 & 2 & 1 \\ 6 & 9 & 4 & 6 & 2 & 3 \end{bmatrix}$$

Observe that $\boldsymbol{A} \otimes \boldsymbol{B} \neq \boldsymbol{B} \otimes \boldsymbol{A}$.

APPENDIX IV
DETERMINATION OF (31)

This Appendix provides the proof of the determination of matrix (31). At the i-th step of the implicit trapezoidal method for DDAE, one has to solve the following nonlinear system:

$$\begin{aligned}\boldsymbol{0} &= \boldsymbol{x}^{(i)} - \boldsymbol{x}(t-\Delta t) - 0.5\Delta t(\boldsymbol{f}^{(i)} + \boldsymbol{f}(t-\Delta t)) \\ \boldsymbol{0} &= \boldsymbol{g}^{(i)} \\ \boldsymbol{0} &= \boldsymbol{\phi}^{(i)} = \hat{\boldsymbol{x}}(\boldsymbol{\alpha}(\boldsymbol{x}^{(i)}, t)) - \boldsymbol{x}_d^{(i)} \\ \boldsymbol{0} &= \boldsymbol{\psi}^{(i)} = \hat{\boldsymbol{y}}(\boldsymbol{\beta}(\boldsymbol{y}^{(i)}, t)) - \boldsymbol{y}_d^{(i)}\end{aligned} \tag{50}$$

where $\boldsymbol{x}(t-\Delta t)$ and $\boldsymbol{f}(t-\Delta t)$ are known vectors determined at the previous step and the unknowns are $\boldsymbol{x}^{(i)}$, $\boldsymbol{y}^{(i)}$, $\boldsymbol{x}_d^{(i)}$ and $\boldsymbol{y}_d^{(i)}$. The solution of (50) can be obtained using the Newton-Raphson's method and its differentiation leads to (27), as follows:

$$\begin{bmatrix} \boldsymbol{0} \\ \boldsymbol{0} \\ \boldsymbol{0} \\ \boldsymbol{0} \end{bmatrix} = \begin{bmatrix} \boldsymbol{I}_n - 0.5\Delta t\boldsymbol{f}_{\boldsymbol{x}}^{(i)} & -0.5\Delta t\boldsymbol{f}_{\boldsymbol{y}}^{(i)} & -0.5\Delta t\boldsymbol{f}_{\boldsymbol{x}_d}^{(i)} & -0.5\Delta t\boldsymbol{f}_{\boldsymbol{y}_d}^{(i)} \\ \boldsymbol{g}_{\boldsymbol{x}}^{(i)} & \boldsymbol{g}_{\boldsymbol{y}}^{(i)} & \boldsymbol{g}_{\boldsymbol{x}_d}^{(i)} & \boldsymbol{0} \\ \boldsymbol{\phi}_{\boldsymbol{x}}^{(i)} & \boldsymbol{0} & \boldsymbol{\phi}_{\boldsymbol{x}_d}^{(i)} & \boldsymbol{0} \\ \boldsymbol{0} & \boldsymbol{\psi}_{\boldsymbol{y}}^{(i)} & \boldsymbol{0} & \boldsymbol{\psi}_{\boldsymbol{y}_d}^{(i)} \end{bmatrix} \begin{bmatrix} \Delta\boldsymbol{x}^{(i)} \\ \Delta\boldsymbol{y}^{(i)} \\ \Delta\boldsymbol{x}_d^{(i)} \\ \Delta\boldsymbol{y}_d^{(i)} \end{bmatrix} \tag{51}$$

Taking into account that $\boldsymbol{x}_d^{(i)}$ and $\boldsymbol{y}_d^{(i)}$ are explicit functions of $\boldsymbol{x}^{(i)}$, $\boldsymbol{y}^{(i)}$ and t, one can manipulate (27) in order to obtain (31), in fact, from (23) and (24):

$$\begin{aligned}\Delta\boldsymbol{x}_d^{(i)} &= \boldsymbol{\phi}_{\boldsymbol{x}}^{(i)}\Delta\boldsymbol{x}^{(i)} \\ \Delta\boldsymbol{y}_d^{(i)} &= \boldsymbol{\psi}_{\boldsymbol{y}}^{(i)}\Delta\boldsymbol{y}^{(i)}\end{aligned} \tag{52}$$

Hence, substituting (52) into (51) leads to (31).

REFERENCES

[1] A. Bellen, N. Guglielmi, and A. E. Ruehli, "Methods for Linear Systems of Circuit Delay Differential Equations of Neutral Type," *IEEE Transactions on Circuits and Systems - I: Fundamental Theory and Applications*, vol. 46, no. 1, pp. 212–216, Jan. 1999.

[2] S. Oucheriah, "Exponential Stabilization of Linear Delayed Systems Using Sliding-Mode Controllers," *IEEE Transactions on Circuits and Systems - I: Fundamental Theory and Applications*, vol. 50, no. 6, pp. 826–830, Jun. 2003.

[3] B. Liu and H. J. Marquez, "Uniform Stability of Discrete Delay Systems and Synchronization of Discrete Delay Dynamical Networks via Razumikhin Technique," *IEEE Transactions on Circuits and Systems - I: Regular Papers*, vol. 55, no. 9, pp. 2795–2805, Oct. 2008.

[4] X. Zhang and Q. Han, "A New Stability Criterion for a Partial Element Equivalent Circuit Model of Neutral Type," *IEEE Transactions on Circuits and Systems - II: Express Briefs*, vol. 56, no. 10, pp. 798–802, Oct. 2009.

[5] V. Venkatasubramanian, H. Schattler, and J. Zaborszky, "A Time-delay Differential-algebraic Phasor Formulation of the Large Power System Dynamics," in *IEEE International Symposium on Circuits and Systems (ISCAS)*, vol. 6, London, England, May 1994, pp. 49–52.

[6] H. Wu and G. T. Heydt, "The Impact of Time Delay on Robust Control Design in Power Systems," in *Proceedings of the IEEE PES Winter Meeting*, vol. 2, Chicago, Illinois, 2002, pp. 1511–1516.

[7] H. Wu, K. S. Tsakalis, and G. T. Heydt, "Evaluation of Time Delay Effects to Wide-Area Power System Stabilizer Design," *IEEE Transactions on Power Systems*, vol. 19, no. 4, pp. 1935–1941, Nov. 2004.

[8] I. A. Hiskens, "Time-Delay Modelling for Multi-Layer Power Systems," in *Proceedings of the IEEE International Symposium on Circuits and Systems (ISCAS)*, vol. 3, Bangkok, Thailand, May 2003, pp. 316–319.

[9] S. Ayasun and C. O. Nwankpa, "Probability of Small-Signal Stability of Power Systems in the Presence of Communication Delays," in *International Conference on Electrical and Electronics Engineering (ELECO)*, vol. 1, Bursa, Turkey, 2009, pp. 70–74.

[10] H. Jia, N. Guangyu, S. T. Lee, and P. Zhang, "Study on the Impact of Time Delay to Power System Small Signal Stability," in *Proceedings of the IEEE MELECON*, Benalmádena, Spain, May 2006, pp. 1011–1014.

[11] H. Jia, X. Cao, X. Yu, and P. Zhang, "A Simple Approach to Determine Power System Delay Margin," in *Proceedings of the IEEE PES General Meeting*, Montreal, Quebec, 2007, pp. 1–7.

[12] R. M. Corless, G. H. Gonnet, D. E. G. Hare, D. J. Jeffrey, and D. E. Knuth, "On the Lambert W Function," *Advances in Computational Mathematics*, vol. 5, pp. 329–359, 1996.

[13] K. Engelborghs and D. Roose, "Bifurcation Analysis of Periodic Solutions of Neutral Functional Differential Equations: A Case Study," *International Journal on Bifurcation and Chaos in Applied Sciences and Engineering*, vol. 8, no. 10, pp. 1889–1905, Aug. 1998.

[14] O. Diekmann, S. A. van Gils, S. M. Verduyn Lunel, and H. O. Walther, *Delay EquationsFunctional, Complex and Nonlinear Analysis*. New York: Springer, 1995, vol. 110.

[15] K. Engelborghs and D. Roose, "Numerical Computation of Stability and Detection of Hopf Bifurcations of Steady-state Solutions of Delay Differential Equations," *Advances in Computational Mathematics*, vol. 10, no. 3-4, pp. 271–289, 1999.

[16] K. Engelborghs, T. Luzyanina, and D. Roose, "Numerical Bifurcation Analysis of Delay Differential Equations Using DDE-BIFTOOL," *ACM Transactions on Mathematical Software*, vol. 1, no. 1, pp. 1–21, 2000.

[17] K. Engelborghs and D. Roose, "On Stability of LMS Methods and Characteristic Roots of Delay Differential Equations," *SIAM Journal of Numerical Analysis*, vol. 40, no. 2, pp. 629–650, 2002.

[18] A. Bellen and S. Maset, "Numerical Solution of Constant Coefficient Linear Delay Differential Equations as Abstract Cauchy Problems," *Numerische Mathematik*, vol. 84, pp. 351–374, 2000.

[19] A. Bellen and M. Zennaro, *Numerical Methods for Delay Differential Equations*. Oxford: Oxford Science Publications, 2003.

[20] D. Breda, S. Maset, and R. Vermiglio, "Pseudospectral Approximation of Eigenvalues of Derivative Operators with Non-local Boundary Conditions," *Applied Numerical Mathematics*, vol. 56, pp. 318–331, 2006.

[21] S. Qiang, A. Haiyun, J. Hongjie, Y. Xiaodan, W. Chenshan, W. Wei, M. Zhiyu, Z. Yuan, Z. Jinli, and L. Peng, "An Improved Power System Stability Criterion with Multiple Time Delays," in *Proceedings of the IEEE PES General Meeting*, Calgary, Alberta, 2009, pp. 1–7.

[22] L. Ting, W. Min, H. Yong, and C. Weihua, "New Delay-dependent Steady State Stability Analysis for WAMS Assisted Power System," in *Proceedings of the 29th Chinese Control Conference*, Beijing, China, Jul. 2010, pp. 29–31.

[23] M. S. Mahmoud, *Robust Control and Filtering for Time-Delay Systems*. New York: Marcel Dekker, 2000.

[24] M. Wu, Y. He, and J. She, *Stability Analysis and Robust Control of Time-Delay Systems*. New York: Springer, 2010.

[25] W. Yao, L. Jiang, Q. H. Wu, J. Y. Wen, and S. J. Cheng, "Delay-Dependent Stability Analysis of the Power System with a Wide-Area Damping Controller Embedded," *IEEE Transactions on Power Systems*, vol. 26, no. 1, pp. 233–240, Feb. 2011.

[26] I. A. Hiskens, "Power System Modeling for Inverse Problems," *IEEE Transactions on Circuits and Systems - I: Regular Papers*, vol. 51, no. 3, pp. 539–551, Mar. 2004.

[27] W. Michiels and S. Niculescu, *Stability and Stabilization of Time-Delay Systems*. Philadelphia: SIAM, 2007.

[28] D. Breda, "Solution Operator Approximations for Characteristic Roots of Delay Differential Equations," *Applied Numerical Mathematics*, vol. 56, pp. 305–317, 2006.

[29] F. Milano, *Power System Modelling and Scripting*. London: Springer, 2010.

[30] IEEE Working Group on Computer Modelling of Excitation Systems, "Excitation System Models for Power System Stability Studies," *IEEE Transactions on Power Apparatus and Systems*, vol. 100, no. 2, pp. 494–509, Feb. 1981.

[31] D. C. Lee (Chair), "IEEE Recommended Practice for Excitation System Models for Power System Stability Studies," IEEE Standards Board, Tech. Rep., Mar. 1992, iEEE std 421.5-1992.

[32] K. J. Runtz, A. S. A. Farag, D. W. Huber, G. S. Hope, and O. P. Malik, "Digital Control Scheme for a Generating Unit," *IEEE Transactions on Power Apparatus and Systems*, vol. PAS-92, no. 2, pp. 478–483, March/April 1973.

[33] O. P. Malik, G. S. Hope, and D. W. Huber, "Design and Results of a Software Based Digital AVR," *IEEE Transactions on Power Apparatus and Systems*, vol. PAS-93, no. 2, pp. 634–642, March/April 1976.

[34] C. Goldemberg, E. Lorenzetti Pellini, and S. Ura, "Real Time Simulator for Hydro-Generator Excitation Sytems," in *Proceedings of the IEEE International Symposium on Industrial Electronics (ISIE)*, Montreal, Canada, Jul. 2006, pp. 2585–2590.

[35] S. Mohr and T. Bosselmann, "A High Dynamic Magnetooptic Current Transformer with Advanced Signal Processing," *IEEE Sensors Journal*, vol. 3, no. 1, pp. 87–94, Feb. 2003.

[36] C. A. Cañizares, "Voltage Stability Assessment: Concepts, Practices and Tools," IEEE/PES Power System Stability Subcommittee, Final Document, Tech. Rep., Aug. 2002, available at http://www.power.uwaterloo.ca.

[37] R. Zárate-Miñano, F. Milano, and A. J. Conejo, "An OPF Methodology to Ensure Small-Signal Stability, IEEE Transactions on Power Systems," *IEEE Transactions on Power Systems*, 2010, in press.

[38] F. Milano, "An Open Source Power System Analysis Toolbox," *IEEE Transactions on Power Systems*, vol. 20, no. 3, pp. 1199–1206, Aug. 2005.

[39] E. Anderson, Z. Bai, C. Bischof, S. Blackford, J. Demmel, J. Dongarra, J. D. Croz, A. Greenbaum, S. Hammarling, A. McKenney, and D. Sorensen, *LAPACK Users' Guide, Third Edition*. Philadelphia, PA: SIAM, 1999, available at http://www.netlib.org/lapack/lug/.

[40] ARPACK software, available at http://www.caam.rice.edu/software/ARPACK/.

[41] "Available Transfer Capability Definition and Determination," NERC, USA, Tech. Rep., 1996.

[42] L. N. Trefethen, *Spectral Methods in Matlab*. Philadelphia: SIAM, 2000.

[43] A. J. Laub, *Matrix Analysis for Scientists and Engineers*. Philadelphia: SIAM, 2005.

Federico Milano (Senior Member '09) received from the University of Genoa, Italy, the Electrical Engineering degree and the Ph.D. degree in 1999 and 2003, respectively. From 2001 to 2002 he worked at the University of Waterloo, Canada as a Visiting Scholar. He is currently an associate Professor at the University of Castilla-La Mancha, Ciudad Real, Spain. His research interests include voltage stability, electricity markets and computer-based power system modeling and analysis.

Marian Anghel received a M.Sc. degree in Engineering Physics from the University of Bucharest, Romania, in 1985 and a Ph.D. degree in Physics from the University of Colorado at Boulder, USA, in 1999. He is currently a technical staff member with the Computer, Computational and Statistical Sciences Division at the Los Alamos National Laboratory, Los Alamos, USA. His research interests include statistical learning, forecasting, and inference algorithms, model reduction and optimal prediction in large scale dynamical systems, and infrastructure modeling and analysis.